Electron Density as a Descriptor of Thermal Molecular Size

John Bentley†

Radiation Laboratory, University of Notre Dame, Notre Dame, Indiana 46556-0579

Received: June 16, 2000; In Final Form: August 15, 2000

A quantitative relationship is developed between repulsive intermolecular potential surfaces and molecular electron density contours, using the helium atom as a probe. For a variety of small neutral molecules and anions, the molecular surface consistent with approach of a helium atom at a temperature of 298 K is identified with the electron density contour at 0.0033 ± 0.0005 au. This gives a prescription for molecular size and shape that is expected to be useful for cavities in solution and other applications.

Introduction

The concept of the size and shape of a molecule is intuitively clear to most chemists, but unique specification of the size and shape of any molecule is unrealizable. With an electron density that decays exponentially, an isolated molecule has no natural border. Experimental approaches to size and shape, such as crystal structures, inversion of intermolecular scattering data, or liquid diffraction experiments, rely on probing the interactions of a particular molecule with its neighbors. Since each method probes a somewhat different aspect of the molecule and its response to its environment, it is not surprising that descriptions of size and shape vary with the probe. It is worthwhile to keep in mind that the environment is an essential part of any characterization of molecular size and shape.

Notwithstanding that fact, many of our models for describing molecular dimensions are based on properties of the isolated molecule or its constituent atoms. At present, the most widespread such procedure seems to be the van der Waals envelope.[1] Each atom sits at the center of a sphere characterized by an atomic van der Waals radius, and the molecular envelope is the outer surface obtained from the union of all the atomic spheres. There are several commonly used sets (e.g., refs 2, 3, and 4) of van der Waals or related radii. Various refinements have been advanced, such as the dependence of the atomic radius on the charge state of the atom[5] or the use of solvent probe spheres to avoid derivative discontinuities in the molecular surface.[1]

A different approach is to describe the molecule by a particular contour of its total electron density. This has the advantages over van der Waals methods that (i) one need only specify a single contour rather than a list of atomic radii, (ii) the resulting molecular surface is naturally continuous, and (iii) it is already fully adapted to the charge states of atoms within the molecule. Its disadvantage is that one must calculate the properties of the full molecule rather than sum a set of atomic properties. The idea of using electron density in this way has a long history. Bader, Henneker, and Cade,[6] for instance, proposed using the 0.002 au contour, pointing out that this value gave molecular dimensions consistent with those inferred from gas-phase thermodynamic data and crystal X-ray diffraction studies of diatomics such as N_2 and O_2. (1 atomic unit (au) of electron density = 1 electron per bohr^3; 1 bohr (a_0) = 0.052 917 7 nm.)

In the present study we attempt to isolate one specific contribution to molecular size and shape, namely, the repulsion arising from overlap of the electron densities of neighboring molecules. Of course, it is impossible to exactly partition a molecular interaction in this way, but it is possible to choose systems in which the desired contribution predominates. For this purpose, the helium atom in its ground state is the best probe. It is small, spherical, and neutral, lacks electron spin, and has relatively low polarizability. These properties minimize the contributions from electrostatic, inductive, and dispersion interactions, eliminate the possibility of chemical reactions, and preclude most steric effects. From an examination of helium interacting with a number of molecules, we make an explicit, quantitative connection between the molecular electron density and the energetics of thermal collisions between a molecule and its neighbors.

There have been prior studies in which electron density has played an important role in describing molecular interactions, and others in which helium has been used to probe molecules. In early work by Gordon and Kim,[7] the density function was central to the computation of the interaction energy between pairs of rare gas atoms. More recently, Stone's group[8] has developed a procedure for predicting intermolecular potential energy surfaces that depends on the overlap of electron density functions to produce the repulsive part of the surface. Stone and Tong[9] have predicted interaction energies between various molecules A and B by computing the interaction energies of A and B with helium and using combining rules to determine the repulsive part of the AB potential surface. Badenhoop and Weinhold[10,11] have reported a procedure utilizing natural bond orbitals, in which van der Waals radii are derived for molecules interacting with helium or neon by noting the distances at which the repulsive energy equals kT (T = 298 K) and using a combining rule.

This earlier work emphasizes the fact that the shape of the total molecular electron density correlates with the shape of the molecule's potential surface for interaction with a suitable probe, and provides several methods for using the electron density to predict (part of) the intermolecular potential. Here we are concerned with using the intermolecular potential to identify electron density contours that are characteristic of specific

† E-mail: bentley.1@nd.edu.

10.1021/jp0021749 CCC: $19.00
Published on Web 09/28/2000

repulsive interactions. This work extends a theme introduced by Bone and Bader[12] and amplified by us,[13] in which regularities of the intermolecular electron density in van der Waals complexes were displayed and examined. In the present work the correlation has been extended to repulsive interactions and made explicit: Particular repulsive interaction energies are associated with particular contours of electron density.

Method and Illustrative Results for He−HF

The general idea behind this work is that the molecular electron density is responsible for determining a molecule's size and shape, by virtue of excluding other molecules from occupying the same region of space through the repulsion interaction arising from overlapping electron densities. Of course, various interaction terms contribute to the intermolecular potential energy, and it is no easy task to resolve them. It is preferable to examine molecular interactions that maximize the effect we want to measure. As stated in the Introduction, the helium atom seems the best available probe, owing to its relative inability to engage in attractive interactions. Other elements in the rare gas period are progressively larger and more polarizable, presenting the possibility of gradually increasing the roles played by dispersion, induction, and steric interactions. At present, however, we restrict our attention to helium.

The general scheme is as follows: First, the potential surface of the probe−molecule interaction (V_{PM}) is explored, and contours on the energy surface are identified that correspond to $V_{PM} = kT$. An energy contour obtained in this way defines a molecular volume from which probe nuclei are (on average) excluded at the specified temperature. The surface that bounds this volume is similar to what Richards[1] calls the solvent accessible surface (SAS), assigning the probe atom the role of solvent. The SAS is the surface described by the center of a solvent sphere rolling over the van der Waals surface of the target molecule, whereas the present surface is based on an energy criterion. For the present purposes, a more useful surface would be one that represents the boundary between the molecule and the probe.

Bader has presented a quantum theory of atoms in molecules[14] in which the boundaries between atoms are those surfaces through which the gradient of the electron density has zero flux. This surface is defined for repulsively interacting atoms as well as for atoms chemically bound to one another. The (3, −1) stationary point in the electron density between atoms in a molecule, referred to as the bond critical point (BCP), contains considerable information about the nature and strength of the bond. It is also the point of maximum density on the surface that separates the two atoms. If the helium atom is rolled around the exterior of a molecule at a distance corresponding to a particular repulsive energy contour, the surface generated by the BCPs provides a well-defined boundary between the molecule and a helium bath at the specified temperature. We will refer to this surface as the exclusion surface of molecule M at temperature *T*.

Finally, we need to relate the exclusion surface, which is characteristic of a family of collision complexes, to the electron density of the isolated target molecule. This is done by a computational experiment, simply noting where the exclusion surface intersects the electron density function of the isolated molecule. Computational details are as follows.

The probe atom is moved toward the molecule of interest along a number of straight-line trajectories. Trajectories are chosen to be essentially collinear with the gradient of the molecular electron density; thus, most trajectories point toward one of the molecular nuclei. Occasionally, the midpoint of a bond or other nonnuclear point is found to be the most appropriate terminus of a trajectory. The molecular geometry is not allowed to vary as the probe atom approaches. The energy is computed at regular intervals along these lines, using the RHF/6-311+G(d,p) and MP2/6-311+G(d,p) levels of theory as implemented in the GAUSSIAN-94 program suite.[15] The intermolecular potential energy V_{PM} is determined by application of the counterpoise correction.[16] The intermolecular potential energy is interpolated to locate those distances at which the energy is equivalent to temperatures of 77, 298, and 398 K (i.e., $V_{PM}(\boldsymbol{R}^T) = kT$). This is depicted in Figure 1 for the approach of helium to hydrogen fluoride, where the 77, 298, and 398 K energy contours from the MP2 calculation are displayed. (On the scale of the figure, the corresponding RHF results are practically indistinguishable from those of MP2.)

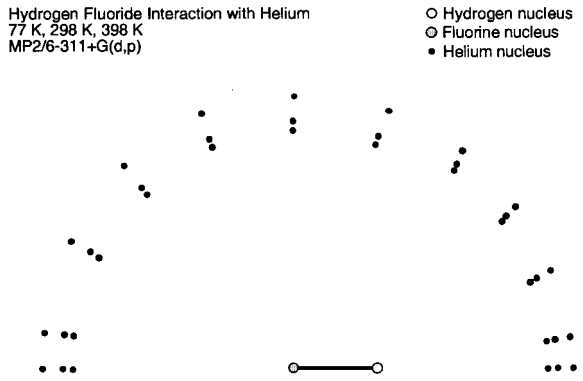

Figure 1. Potential energies for approach of helium to hydrogen fluoride. The outermost ring of points corresponds to a repulsive energy equivalent to 77 K; the inner rings are 298 and 398 K. The H−F internuclear distance is 0.896 Å.

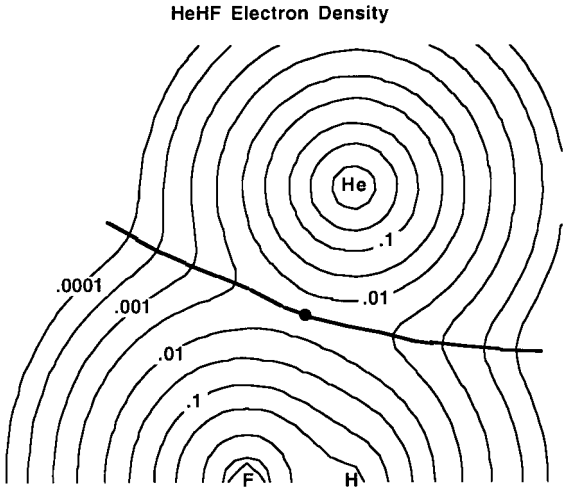

Figure 2. Molecular electron density in the nuclear plane for the He−HF interaction at 298 K, employing MP2/6-311+G(d,p) wave functions. The bond critical point is shown as a solid circle, and the surface separating helium from hydrogen and fluorine as a heavy line. Electron densities increase in logarithmic steps. The outermost is 0.0001 au, and the next one is 0.0003 au.

Once those intermolecular geometries that lie on the desired repulsive contour have been identified, the wave function of the collision complex is calculated at those points. Bond critical points between the probe and the molecule are determined for each interaction geometry using the program EXTREME from the AIMPAC suite.[17] In Figure 2, the electron density function in the nuclear plane is shown for a particular direction of helium approach to HF, and the BCP and probe−molecule

TABLE 1: Excluded Surface Electron Densities (in au) around Hydrogen Fluoride

	RHF			MP2		
	398 K	298 K	77 K	398 K	298 K	77 K
HFHe angle (deg)						
180	0.004 88	0.004 04	0.001 63	0.005 44	0.004 59	0.002 13
170	0.004 89	0.004 04	0.001 63	0.005 44	0.004 58	0.002 12
150	0.004 92	0.004 06	0.001 61	0.005 42	0.004 54	0.002 01
130	0.004 91	0.004 03	0.001 56	0.005 29	0.004 39	0.001 86
110	0.004 80	0.003 93	0.001 51	0.005 07	0.004 19	0.001 74
90	0.004 56	0.003 73	0.001 45	0.004 76	0.003 93	0.001 65
70	0.004 22	0.003 46	0.001 38	0.004 40	0.003 65	0.001 58
FHHe angle (deg)						
180	0.005 22	0.004 44	0.002 43	0.006 35	0.005 44	0.003 23
170	0.005 22	0.004 44	0.002 41	0.006 33	0.005 45	0.003 21
150	0.005 19	0.004 39	0.002 28	0.006 14	0.005 28	0.002 96
130	0.004 91	0.004 11	0.001 93	0.005 57	0.004 72	0.002 41
110	0.004 35	0.003 58	0.001 25	0.004 67	0.003 89	0.001 57
average value	0.004 84	0.004 02	0.001 76	0.005 41	0.004 55	0.002 21
standard dev	0.000 32	0.000 32	0.000 41	0.000 63	0.000 60	0.000 61

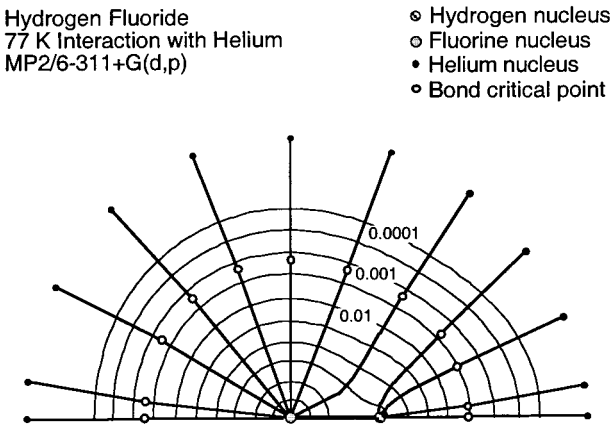

Figure 3. Bond critical points and bond paths from the 77 K interaction of He with HF, superimposed on the MP2/6-311+G(d,p) electron density of the hydrogen fluoride molecule. Electron density values are as in Figure 2.

surface are indicated. The electron density of the target molecule, $\rho_M(\boldsymbol{R}^{BCP,T})$, is calculated at the position of the BCP. This is represented in Figure 3, where the BCPs for the 298 K interactions are projected onto the electron density contours of the isolated HF molecule. By averaging over all $\rho_M(\boldsymbol{R}^{BCP,T})$ for a given molecule, we obtain the average electron density on the exclusion surface. With certain exceptions, we find that the magnitude of the exclusion surface electron density varies little within a molecule and between molecules, at a given temperature. Magnitudes of the exclusion surface electron densities involved in the helium−hydrogen fluoride interaction are collected in Table 1. The extent of variation of $\rho_M(\boldsymbol{R}^{BCP,T})$ can be judged from the table.

Some comment is necessary about the need for calculations with RHF and MP2. An intermolecular interaction computed at the Hartree−Fock level is capable of describing the overlap repulsion and electrostatic components of the interaction, but not the dispersion component. Thus RHF energies would seem to isolate just the component we are looking for. On the other hand, the electron density of the isolated molecule is slightly altered if the wave function of the molecule is correlated, so one obtains a better description of the isolated molecule at the cost of adding dispersion and inductive components to the description of the complex. With helium as the probe atom, these attractive components are modest in size. The effect seen in helium will serve as a baseline for similar effects in future studies in which the much more polarizable argon atom will be used as the probe.

In the helium−molecule complexes, at those distances for which the molecular electron density is in the range 0.001−0.005 au, the MP2 density is generally slightly larger than the RHF density at the same point. Also, it is generally found that the repulsive wall lies at shorter internuclear distances for the MP2 potential energy than for the RHF energy. Both these factors contribute to a larger value of the BCP density $\rho_M{}^{BCP}$ from MP2 than from RHF. However, this increase does not affect any of the trends observed.

In our previous study of van der Waals complexes and other bound species, considerable use was made of the observation[12,13] that the total density at the BCP, $\rho_{AB}{}^{BCP}(\boldsymbol{R}^{BCP,T})$, can be partitioned into molecular contributions from the component systems A and B:

$$\rho_{AB}{}^{BCP}(\boldsymbol{R}^{BCP,T}) \approx \rho_A(\boldsymbol{R}^{BCP,T}) + \rho_B(\boldsymbol{R}^{BCP,T}) \qquad (1)$$

$\rho_{AB}{}^{BCP}$ was calculated from the wave function of the van der Waals complex. The terms on the right side of eq 1 were calculated from the wave functions of the isolated molecules. When the same relationship is applied to the helium−molecule collision complexes reported here, it is found that $\rho_{HeM}{}^{BCP}$ estimated by eq 1 is consistently overestimated relative to its calculated value, by an average of 2% at 77 K, 5% at 298 K, and 6% at 398 K. This is illustrated in Figure 4, in which the difference density $\Delta\rho(\mathbf{r}) = \rho_{HeHF}(\mathbf{r}) - \rho_{He}(\mathbf{r}) - \rho_{HF}(\mathbf{r})$ is shown for a particular HeHF geometry. The helium atom is polarized in the direction of the molecular dipole moment, and the molecule is polarized toward the helium, but the magnitudes of these differences are quite small. The greatest contour on the Figure is 0.003 au, near the fluorine nucleus. In the vicinity of the BCP, $\Delta\rho$ is on the order of −0.0002 au, roughly 1/40 of the value of $\rho_{HeHF}{}^{BCP}$. Because of the systematic error that it would involve, eq 1 is not used to compute any quantities reported here, although it does still provide an approximate relationship between the density at the BCP and the densities of the isolated probe and molecule.

Results

We have examined the interactions of helium with the neutral molecules methane, ammonia, water, hydrogen fluoride, neon, formaldehyde, hydrogen cyanide, methyl chloride, and benzene,

TABLE 2: Average Excluded Surface Electron Densities (in au) around a Series of Molecules at Various Temperatures

	RHF			MP2		
molecule	398 K	298 K	77 K	398 K	298 K	77 K
Ne	0.004 53	0.003 74	0.001 54	0.004 85	0.004 05	0.001 79
HF	0.004 84 (32)[a]	0.004 02 (32)	0.001 76 (41)	0.005 41 (63)	0.004 55 (60)	0.002 21 (61)
H_2O	0.004 26 (53)	0.003 53 (46)	0.001 50 (27)	0.004 72 (76)	0.003 98 (69)	0.001 90 (48)
NH_3	0.003 68 (56)	0.003 05 (48)	0.001 26 (26)	0.004 05 (80)	0.003 40 (71)	0.001 57 (47)
CH_4	0.003 50 (36)	0.002 91 (29)	0.001 26 (9)	0.004 02 (37)	0.003 41 (29)	0.001 69 (11)
HCN	0.003 95 (62)	0.003 32 (57)	0.001 54 (45)	0.004 24 (32)	0.003 59 (26)	0.001 75 (13)
H_2CO	0.004 06 (48)	0.003 37 (39)	0.001 38 (12)	0.004 65 (43)	0.003 95 (36)	0.001 96 (18)
C_6H_6	0.003 35 (57)	0.002 76 (43)	0.001 17 (17)	0.00419 (51)	0.003 60 (37)	0.002 01 (21)
CH_3Cl	0.003 58 (30)	0.002 99 (24)	0.001 33 (10)	0.004 05 (62)	0.003 55 (33)	0.001 88 (39)
F^-	0.004 91	0.004 05	0.001 89	0.004 26	0.003 48	0.001 53
OH^-	0.003 96 (77)	0.003 27 (71)	0.001 46 (47)	0.003 76 (94)	0.003 10 (85)	0.001 39 (55)
HCO_2^-	0.003 63 (80)	0.003 02 (70)	0.001 31 (32)	0.003 77 (73)	0.003 17 (60)	0.001 44 (34)
Na^+	0.007 29	0.006 90	0.005 60	0.007 55	0.007 18	0.005 69
NH_4^+	0.005 60 (98)	0.004 96 (88)	0.003 23 (65)	0.006 76 (129)	0.006 08 (119)	0.004 38 (95)
$N(CH_3)_4^+$	0.003 32 (82)	0.002 86 (66)	0.001 42 (25)	0.004 17 (95)	0.003 65 (80)	0.002 21 (36)
average (excluding cations)	0.004 02 (53)	0.003 34 (46)	0.001 45 (26)	0.004 34 (59)	0.003 65 (51)	0.001 75 (34)

[a] Standard deviations are given in parentheses.

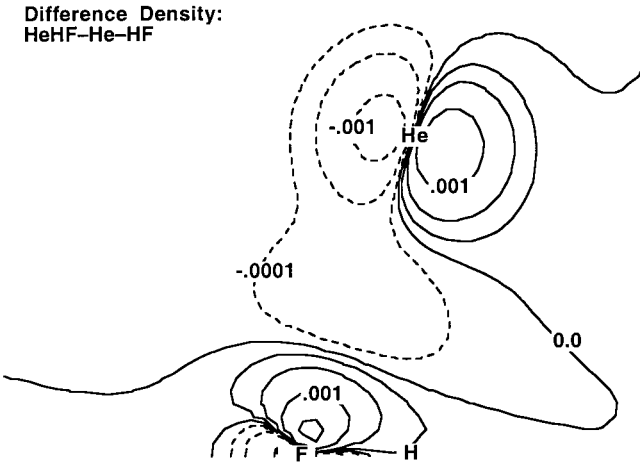

Figure 4. Difference density, $\Delta\rho(\mathbf{r}) = \rho_{HeHF}(\mathbf{r}) - \rho_{He}(\mathbf{r}) - \rho_{HF}(\mathbf{r})$, shown in the same plane and for the same geometry and wave function as in Figure 2. Electron density values are as in Figure 2.

the fluoride, hydroxide and formate anions, and the sodium, ammonium, and tetramethylammonium cations. In each case the number of approaches of the probe to the molecule was sufficient to generate a reasonably complete three-dimensional surface. The average exclusion surface electron densities associated with particular temperatures (i.e., repulsive energies) are collected in Table 2 and depicted in Figure 5.

It is immediately evident that the exclusion surfaces of the various molecules correspond quite closely to particular molecular density contours. This observation applies not only to each molecule but also to comparisons between the molecules. While some variation is apparent in the results, their most interesting feature is the uniformity of the thermal densities. The outstanding exceptions are the sodium and ammonium cations, which have much higher exclusion surface densities than the other molecules examined here. These exceptions will be discussed later.

The exclusion surface densities averaged over the set of molecules studied here are also presented in Table 2. (The cations have been withheld from this average because some of those investigated are qualitatively different from the other molecules studied, as noted above.) The data in Table 2 and Figure 5 indicate that exclusion surfaces are consistent with the following electron density contours (RHF results): 0.001 45 ± 0.000 26 au at 77 K, 0.003 34 ± 0.000 46 au at 298 K, and

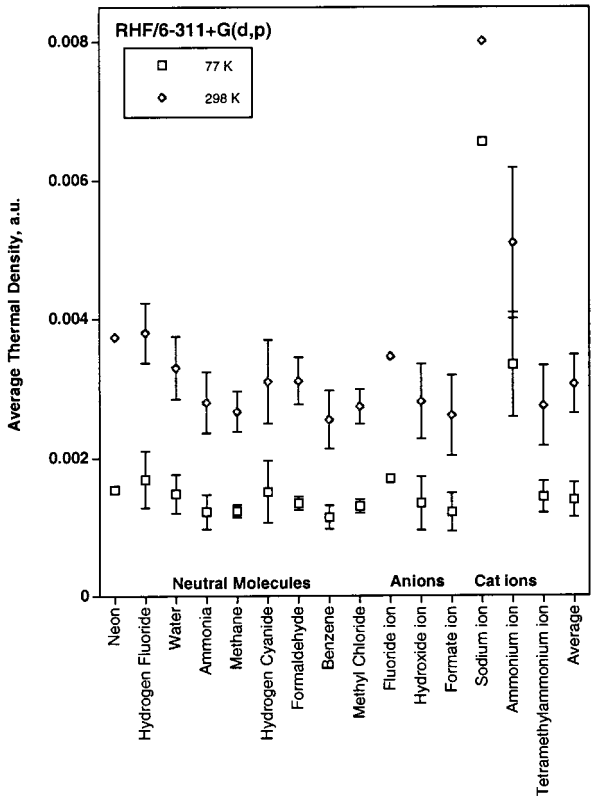

Figure 5. Average exclusion electron densities at two temperatures for 15 molecules. Bars indicate standard deviations of the exclusion electron density within a particular molecule. Data for 398 K have been omitted because they overlap substantially with the 298 K data. The average over neutral and anionic molecules appears as the rightmost entry in the graph.

0.004 02 ± 0.000 53 au at 398 K. MP2 results are roughly 0.0003 au higher at each temperature. The relative standard deviations of 18% at 77 K and 14% at the higher temperatures may seem large at first glance. It must be borne in mind that density varies exponentially with distance, and a shift of 0.1 Å in the position of the exclusion surface can change the corresponding density by ±40%. This sensitivity emphasizes the consistency of the thermal exclusion densities inferred by probing the molecules with a helium atom. The consistency of exclusion densities across a variety of molecules is particularly noticeable in Figure 5.

Limitations and Extension of the Method

To this point we have stressed the uniformity of the exclusion densities across a diverse family of molecules, but closer examination indicates that the deviations from the average, while generally small, are systematic. For the noncationic molecules, positive deviations in exclusion densities occur in the vicinity of hydrogen atoms, and negative deviations are associated with the more electronegative atoms. In the 10-electron hydride sequence, the average density at the 77 K RHF exclusion surface around hydrogen rises from 0.0014 au in methane to 0.0024 au in hydrogen fluoride. This correlates with an increase in the density gradient at the exclusion surface near hydrogen in those molecules. Contrast hydrogen fluoride with the isoelectronic and structurally similar hydroxide anion, in which the 77 K density is only 0.0014 au. In OH^- the density at the exclusion surface around H is characterized by a much smaller gradient (normalized gradient $|\nabla\rho|/\rho = 3.82$ Å^{-1} compared to 4.76 Å^{-1} for HF).

Cationic molecules clearly deviate from the pattern established by neutrals and anions. Comparing methane with ammonium, the average RHF density at the 77 K exclusion surface in the neutral is 0.0013 au, rising to 0.0032 au in the cation. The normalized gradients are 4.28 Å^{-1} in CH_4 and 4.97 Å^{-1} in NH_4^+. In the monatomic, 10-electron series F^-, Ne, Na^+, the respective 77 K thermal RHF densities are 0.0019, 0.0015, and 0.0056 au. In sodium cation as well as in ammonium, the helium is probing nuclei that are substantially deprived of valence electron density. To examine a system in which the positive charge is expected to be less localized on atoms near the molecular surface, we considered the tetramethylammonium cation. The average 77 K RHF density for $N(CH_3)_4^+$ was 0.0014 au, in agreement with the average values for neutrals and anions. In molecules with more contracted valence densities (larger gradients), the probe is seen to penetrate further before experiencing a given repulsive potential.

The results of the previous paragraph indicate the reason for the good correlation between electron density and repulsive energy: Most closed-shell molecules in equilibrium configurations have a normalized density gradient in the van der Waals region of 3.5−4.5 Å^{-1}(see Table 2 of ref 13), so from the probe's point of view they appear essentially the same. Cations hold their electrons more tightly, as reflected in larger density gradients. On this basis, we anticipate that anions or other molecules with very diffuse electron densities (and small exponents) will have thermal exclusion densities below those of Table 2. This is confirmed by calculations on the hydride anion (H^-), for which RHF and MP2 densities at the 77 K exclusion surface are each 0.0007 au. The values at higher temperatures are likewise half the average values from Table 2. This finding both establishes the limits of the present model and suggests an improvement: In a more complete description, the repulsion energy must be a function of both the electron density and the density gradient at the exclusion surface.

Discussion

Two useful concepts come out of this work. First, the exclusion surface defines the shape and size of a molecule at a specified temperature, with respect to a specified probe, and is uniquely determined once the level of theory is specified. With helium as the probing atom, the variation with respect to level of theory appears slight, as long as an adequate basis set is employed (e.g., valence double-ζ plus diffuse and polarization functions).

Second, the approximation of the exclusion surface by a particular contour of electron density provides a convenient and readily accessible method to incorporate molecular volumes into computational applications. We have shown that this approximation is quite successful as long as the molecule being probed has a "typical" normalized electron density gradient at van der Waals distances, namely, 3.5−4.5 Å^{-1}. Methods for removing this limitation are under consideration.

Because the helium exclusion surface represents the minimal possible interaction with surroundings, it provides a useful starting place from which to measure the contributions of other interactions. An example is the dielectric continuum model of solvation, in which a molecule is placed in a cavity inside a dielectric medium, and the induced polarization of the medium is represented as apparent charge on the surface of the cavity. The cavity is clearly akin to an exclusion surface, in that the dielectric medium representing solvent is excluded. Hitherto the cavity shape has been variously assigned as a sphere, an ellipsoid, a van der Waals surface, or a contour of electron density, on the basis of physical arguments and computational implementations.[18] The present study provides support for the use of density contours in this context and places limits on which contours may be appropriate.

One can generalize to other temperatures below 500 K by using the relationship $d\rho_M(\boldsymbol{R}^{BCP,T})/dT = (6.9 \pm 0.9) \times 10^{-6}$ au K^{-1}. (RHF and MP2 trends are essentially the same for this quantity.) This expression is generated from the combined neutral and anionic thermal densities at 298, 398, and 498 K. These data exhibit linear behavior. The 77 K data fall slightly below this line, owing to the effect of the dispersion attraction at the lower temperature. The standard deviation reflects the variation of $d\rho/dT$ from molecule to molecule.

A semiempirical application of electron densities in the spirit of the present study has recently been reported. Shvartsburg, Liu, Jarrold, and Ho[19] used isodensity contours of silicon ion clusters to predict the mobilities of these ions in helium buffer gas. In this application, cluster shape determined by electron density represents a refinement on the commonly used hard-sphere collision model. Shvartsburg et al. chose values of the electron density that best reproduced Si_7^+ and Si_7^- mobility data, and then used the same parameters for the other cluster ions $Si_n^{\pm}$, $n = 3-20$. They reported that the electron-density-based calculations gave a better overall fit to the mobility data than did the hard-sphere calculations. The density values they arrived at, parametrized for room-temperature mobility data, were 0.003 au for cation clusters and 0.0026 for anions, quite consistent with our 298 K exclusion density reported above. They anticipate that this model will be most accurate when the ion−buffer interaction is dominated by repulsive interactions.

Acknowledgment. Dr. Dan Chipman provided valuable comments on this work. Support of the Office of Basic Energy Sciences of the U.S. Department of Energy is gratefully acknowledged. This is Contribution No. NDRL-4090 from the Notre Dame Radiation Laboratory.

References and Notes

(1) Richards, F. M. *Annu. Rev. Biophys. Bioeng.* **1977**, *6*, 151.
(2) Pauling, L. *The Nature of the Chemical Bond*; Cornell University Press: Ithaca, NY, 1960.
(3) Bondi, A. J. *Phys. Chem.* **1964**, *68*, 441−451.
(4) Gavezotti, A. *J. Am. Chem. Soc.* **1983**, *105*, 5220.
(5) Olivares del Valle, F. J.; Aguilar, M. A.; Contador, J. C. *Chem. Phys.* **1993**, *170*, 161−165.
(6) Bader, R. F. W.; Henneker, W. H.; Cade, P. E. *J. Chem. Phys.* **1967**, *46*, 3341−3363.
(7) Gordon, R. G.; Kim, Y. S. *J. Chem. Phys.* **1972**, *56*, 3122−3133.
(8) Hayes, I. C.; Stone, A. J. *Mol. Phys.* **1984**, *53*, 69−83.
(9) Stone, A. J.; Tong, C.-S. *J. Comput. Chem.* **1994**, *15*, 1377−1392.

(10) Badenhoop, J. K.; Weinhold, F. *J. Chem. Phys.* **1997**, *107*, 5406−5421.

(11) Badenhoop, J. K.; Weinhold, F. *J. Chem. Phys.* **1997**, *107*, 5422−5432.

(12) Bone, R. G. A.; Bader, R. F. W. *J. Phys. Chem.* **1996**, *100*, 10892−10911.

(13) Bentley, J. *J. Phys. Chem. A* **1998**, *102*, 6043−6051.

(14) Bader, R F. W. *Atoms in Molecules. A Quantum Theory*; Clarendon: Oxford, UK, 1994.

(15) Frisch, M. T. I.; Trucks, G. W.; Schlegel, H. B.; Gill, P. M. W.; Johnson, B. G.; Robb, M. A.; Cheeseman, J. R.; Keith, T.; Petersson, G. A.; Montgomery, J. A.; Raghavachari, K.; Al-Laham, M. A.; Zakrzewski, V. G.; Ortiz, J. V.; Foresman, J. B.; Peng, C. Y.; Ayala, P. Y.; Chen, W.; Wong, M. W.; Andres, J. L.; Replogle, E. S.; Gomperts, R.; Martin, R. L.; Fox, D. J.; Binkley, J. S.; Defrees, D. J.; Baker, J.; Stewart, J. P.; Head-Gordon, M.; Gonzalez, C.; Pople, J. A. *Gaussian 94*, Revision B.3; Gaussian, Inc.: Pittsburgh, PA, 1995.

(16) Boys, S. F.; Bernardi, F. *Mol. Phys.* **1970**, *19*, 553

(17) Bader, R. F. W., and associates. *AIMPAC 95*; McMaster University: Hamilton, Ont., 1995. Source code was obtained from the AIMPAC site at the following URL: http://www.chemistry.mcmaster.ca/aimpac/aimpac.html.

(18) Tomasi, J.; Persico, M. *Chem. Rev.* **1994**, *94*, 2027−2094.

(19) Shvartsburg, A. A.; Liu, B.; Jarrold, M. F.; Ho, K.-M. *J. Chem. Phys.* **2000**, *112*, 4517−4526.